IEEE Access
Multidisciplinary | Rapid Review | Open Access Journal

Received March 19, 2020, accepted March 31, 2020, date of publication April 6, 2020, date of current version April 21, 2020.

Digital Object Identifier 10.1109/ACCESS.2020.2985847

Vibration Control of Tie Rod Rotors With Optimization of Unbalanced Force and Unbalanced Moment

YIPENG ZHANG[1], LIDONG HE[1,2], JIANJIANG YANG[2], JIAN WANG[2], AND GANG ZHU[2]

[1]Key Laboratory of Engine Health Monitoring-Control and Networking, Ministry of Education, Beijing University of Chemical Technology, Beijing 100029, China

[2]Beijing Key Laboratory of Health Monitoring and Self-Recovery for High-End Mechanical Equipment, Beijing University of Chemical Technology, Beijing 100029, China

Corresponding author: Lidong He (1963he@ 163.com)

This work was supported in part by the National Science and Technology Major Project of China under Grant 2017-IV-0010-0047.

ABSTRACT This paper proposes a method for optimizing unbalanced force and unbalanced moment of the multistage disk based on sequence quadratic program algorithm to solve the vibration problem of gas turbine tie rod rotor. This method guides the assembly phase of the multistage disks. The influence of unbalanced force and unbalanced moment on the vibration of the tie rod rotor are analyzed based on the characteristics of rotor structure and assembly process. A dynamic model of the unbalanced force and unbalanced moment of the tie rod rotor is established. The sequence quadratic program algorithm is used to optimize multi-dimension of unbalanced force and moment, so the global optimal solution can be obtained. In order to verify the effectiveness of the optimization method proposed in this paper, vibration control experiments are carried out for traditional tie rod rotor and gas turbine tie rod rotor structure. The results show that both unbalanced force optimization and unbalanced moment optimization can control the tie rod rotor vibration effectively, and unbalanced moment optimization is better. Unbalanced moment optimization is used to perform constant speed and speed-up experiment on the gas turbine tie rod rotor structure. At 1200r/min, the maximum vibration reduction of the system is 76.68%. And the vibration has a decrease of 43.3% at the first-order critical speed. The proposed method in this paper can be used not only for the guidance of tie rod rotor assembly of gas turbine, but also for the vibration control during operation.

INDEX TERMS Vibration control, unbalanced force optimization, unbalanced moment optimization, tie rod rotor, assembly.

I. INTRODUCTION

Gas turbines are known as the crown jewel in the machinery manufacturing industry and are widely used in energy, aerospace, power generation and other fields. As the tie rod rotor is the core part of a gas turbine, the vibration of this component directly affects the safe operation of the gas turbine [1], [2]. Unbalanced vibration is a common and main phenomenon in the tie rod rotor system. The main reasons for the imbalance of the system are uneven rotor material, wear, corrosion, and impeller fouling during operation. Imbalance causes the system generate strong vibration, which leads to rotor fracture, bearing wear and other failures. These problems not only reduce the life of a tie rod rotor system but also cause major accidents and serious economic losses. Additionally, the vibration can make loud noise, leading to pose a large health threat to people who work in this environment [3], [4]. Therefore, the unbalanced vibration of tie rod rotor systems should be controlled which is of great significance.

Due to the structural characteristics of a tie rod rotor system, the multistage disks are connected by tie rod bolts. In addition, different disks have different imbalances, so the initial imbalance of each disk is also different. Many scholars have made efforts to solve the problem of the unbalanced vibration in tie rod rotors.

Many different types of methods have been developed in order to solve the unbalanced vibration of the tie rod rotor.

The associate editor coordinating the review of this manuscript and approving it for publication was Jianyong Yao.

A diagnosis monitoring system can predict the possible failures of the rotor system in advance [5]–[8]. In [6] and [7], a monitoring system monitors the bearing condition and can warn the problem timely, but the reliability of the diagnosis still needs to be further improved. At the same time, there exists inconsistencies caused by the diversified data when a condition monitoring system is used in a gas turbine. For the complex working environment of a gas turbine, how to ensure the long-term successful operation of the system still requires time to verify [5], [8]. Friction dampers have been applied to gas turbines [9], [10]. The influence of parameters of the contact area on energy dissipation is considered [10]. But the dampers have a lock-up phenomenon. The model needs to improve to adapt the different friction coefficients of blades. The literature [9] puts forward the limitations of the model. In practical applications, the dampers can only use in the same structure, otherwise they should redesign. This literature also suggests to research the friction dynamics in-depth to predict the behavior of the damper more accurately in the future. Active magnetic bearing is a kind of controllable bearing. It can solve the unbalanced vibration of the rotor system [11]–[16]. GE applies AMB to gas turbines, but due to the complexity of the control system and the component materials in high temperature gas, the engineering application of AMB on gas turbines needs to be verified [16]. An experiment on vibration control of an eccentric rigid rotor with an AMB shows that it has a good effect [11]. But the vibration control model of flexible rotor needs to be established. Some researchers propose a method to find the position of the unbalanced mass and compensate by AMB [12], [13]. However, it does not consider the non-linear factors and the unbalanced control are difficult to guarantee in the case of abnormal measurement data. So, an innovative structure of an AMB combining with gas is designed [14] and an accurate vibration model is set up [15]. For the new structure, it is still unclear about the transient performance in the rotor system [14]. The new model gives a direction of solving beat phenomenon and generalized dynamic stiffness but not verify [15]. For a MIMO non-linear system, an output feedback robust tracking controller is designed [17]. This controller implement improves model compensation, and verifies this controller in the disturbance-free system and disturbance system. The development of output feedback controllers for disturbed nonlinear systems with unknown input delay should be considered in the future. In [18], the author proposes an adaptive feedback controller based on the extended state observer. This controller compensates the nonlinear friction of the hydraulic servo control system and it has verified in a hydraulic system. The controller improves the difficult nonlinear friction problem in the hydraulic system and has a strong practical application value. The remaining nonlinear factors and delay issues will be studied in the next step.

In terms of optimization, the nonlinear sealing force and nonlinear oil film force in the nonlinear seal-bearing-rotor system are studied, and use GA to optimize the stability [19]. The main optimized parameters include the seal radius, seal gap and seal length. However, this algorithm is short of stability in the results and poor multi-dimensional parameter. Through its optimization experiments, there is a fluctuation in the calculated value of the seal radius. In [20], a PSO-OP neural network algorithm for predicting the deviation of concentricity and perpendicularity during the rotor assembly process is proposed, which improves the assembly accuracy. Because of a hybrid of global and local algorithms, it exacerbates the possibility of falling in to local optimal solution. At the same time, the number of nodes determines the accuracy of fitting and the calculation results may deviate from the true results. And in the case of hyperparameters, the particle swarm position coordinates must remain integers. This shortcoming is confirmed in the experiments, and the complexity of the algorithm is self-evident. A literature proposes a hybrid evolution algorithm to solve the large-scale equipment assembly [21]. This algorithm is a combination of the ACO and SA algorithm, which aims to reduce the problem of getting stuck in a local optimal solution. The main problem with this algorithm is that it greatly increases the processing capacity of the computer and reduce some factors during assembly process. It can be seen that the cycle time on assembly is not considered in the experiment. In the signal processing, [22] carries out a vibration signal optimization strategy to increase the accuracy and authenticity of the signal. The PSO optimization scale-transformation stochastic resonance algorithm improves the parameter selection and avoids calculation differences of the SR algorithm. However, the algorithm is prone to difference in the parameters after optimization due to the difference in the noise strength of the initial signal, and the robustness and accuracy are poor. In actual experimental tests, there are still multiple optimization combinations, which leads to the need for further screening of the optimal combination.

In view of the current research status of vibration control, many methods are performed in the process. These methods add some complex devices to the rotor system and increase the structural modification. In this paper, unbalanced force optimization and unbalanced moment optimization are proposed to predict the assembly phase of multistage disks for the tie rod rotor system with unbalance vibration. The advantages of this method consist of the following aspects. It not only can avoid the redesign and transformation of the rotor system, but also can ensure a better match between structural components and control the vibration effectively before the dynamic balancing. Also, this paper applies the SQP algorithm to optimize the rotor system. Compared with the literatures, the superiority of this algorithm lies in the following aspects. It is easy to deal with nonlinear constraint problems and find the global optimal solution accurately. This method can optimize and deal with higher dimensions problems and can ensure the reliability of the results with strong stability. What is more, there is no fitting problem and no initial parameters need to be set which may cause the result distorted. The combination of the two proposed methods can control the vibration of rotor system effectively.

The experimental results are utilized to fully verify the useful of the methods.

The remaining of this paper is structured as follows. Section II establishes the dynamic model of the tie rod rotor system with unbalanced force and moment. The basic principle of the SQP algorithm are presented in Section III. In Section IV, the optimization strategy for tie rod rotor system is set up. Experimental validation results are obtained in Section V. Section VI gives the conclusions of this paper.

II. DYNAMIC MODEL AND FORMULATION

Fig.1. illustrates the structure of tie rod rotor. It is positioned radially through the disk groove and disk boss between two multistage disks. In addition, all of the disks were tightened axially with tie rod bolts.

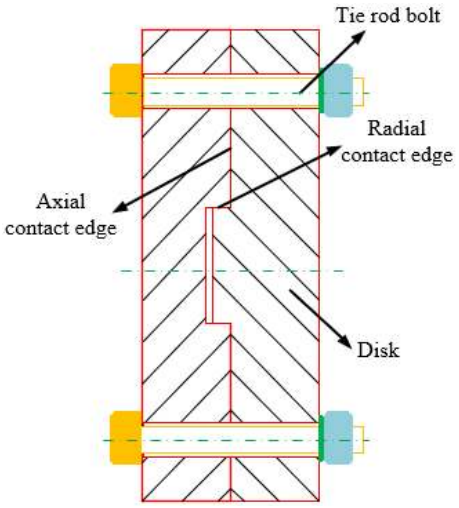

FIGURE 1. The structure of tie rod rotor.

Due to its structural characteristics, the rotor system has multistage disks. There is a certain imbalance of each disk, causing the mass center and the body center not on the same axis. When the rotor system rotates, each disk is accompanied by a certain unbalanced force and unbalanced moment. If these factors are superimposed, the vibration of the system can be increase quickly. Shaft bending and bearing damage are gradually revealed.

Therefore, how to reduce unbalanced force value and unbalanced moment value of the tie rod rotor as close to 0 as possible is a very meaningful research. Unbalanced force is mainly for static balancing, and unbalanced moment is aimed at the state of dynamic balancing.

Besides, both factors have a large influence on the vibration of the tie rod rotor system. Generally, before assembling the tie rod rotor, multistage disks should perform dynamic balancing, respectively. Then assemble them as an integration to test whether the vibration value meets the standard. If the assembly does not meet the standard, multistage disks perform the low-speed dynamic balancing again. The flowchart is shown in Fig. 2.

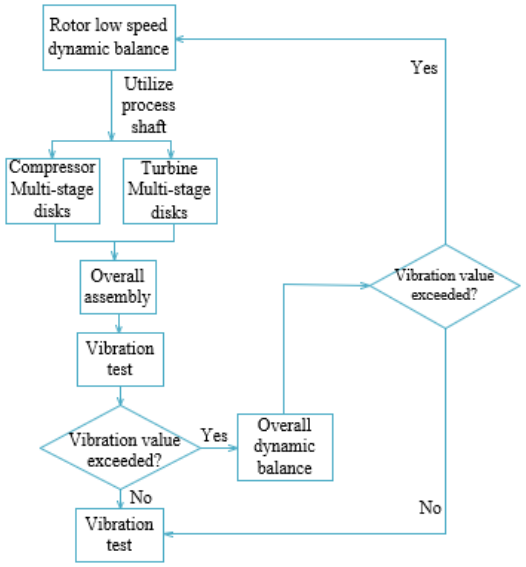

FIGURE 2. Tie rod rotor balancing process.

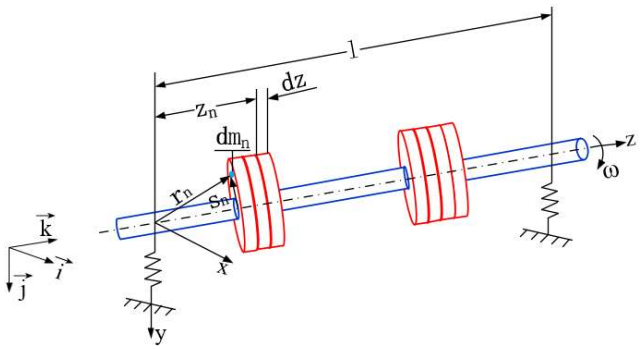

FIGURE 3. The dynamic mode of tie rod rotor system.

As shown in Fig. 3, the dynamic model of a tie rod rotor system is established. Some conditions are assumed. 1) The shaft and disks are uniform and rigid with no deformation. 2) Tie rod bolts remain unchanged while shaft and disks rotate a synchronously. 3) There is the rotational movement only.

The tie rod rotor system rotates at an angular velocity ω. The imbalances in the various disks are $M_1, M_2, M_3 \ldots M_n$, where M_n includes the size and phase of the imbalances. In addition, the distances from the disks to the left support are $z_1, z_2, z_3 \ldots z_n$, respectively [23]–[26].

Take the rotation axis direction as the z-direction and establish an O_{x-y-z} rectangular coordinate system. The imbalance of each disk can be written as

$$\vec{r}_n = x_n\vec{i} + y_n\vec{j} + z_n\vec{k} = \vec{s}_n + z_n\vec{k} \tag{1}$$

where x_n, y_n, z_n are the coordinate components of $\vec{r}_n$. And $\vec{i}$, $\vec{j}$, $\vec{k}$ are unit vectors in all directions; and $\vec{s}_n$ is the projection of $\vec{r}_n$ on the x-y plane.

The speed can be obtained from the differentiation of (1) is

$$\vec{v}_n = \dot{\vec{r}}_n = x_n(d\vec{i}/dt) + y_n(d\vec{j}/dt) + z_n(d\vec{k}/dt) \quad (2)$$

where $d\vec{i}/dt = \vec{\omega}\times\vec{i}$, $d\vec{j}/dt = \vec{\omega}\times\vec{j}$, $d\vec{k}/dt = \vec{\omega}\times\vec{k}$, in which $\vec{\omega} = \omega\vec{k}$, $\vec{\omega}\times\vec{k} = \omega\vec{k}\times\vec{k} = 0$.

The speed can be written as

$$\vec{v}_n = \vec{\omega}\times(x_n\vec{i} + y_n\vec{j} + z_n\vec{k}) = \vec{\omega}\times\vec{r}_n = \vec{\omega}\times\vec{s}_n \quad (3)$$

By differentiating (3), the acceleration can be obtained

$$\vec{a}_n = \dot{\vec{v}}_n = \dot{\vec{\omega}}\times\vec{s}_n + \vec{\omega}\times\dot{\vec{s}}_n = \dot{\omega}\vec{k}\times\vec{s}_n - \omega^2\times\vec{s}_n \quad (4)$$

Due to the different unbalanced masses dm_n in the various disks, the sum of unbalanced forces can be generated

$$d\vec{P} = -\sum_{n=1}^{n}\vec{a}_n dm_n = [(-\dot{\omega}\vec{k}\times) + \omega^2]\sum_{n=1}^{n}\vec{s}_n dm_n \quad (5)$$

Unbalanced force of each disk is a vector perpendicular to the rotation axis z, so the sum of unbalanced moments of the multistage disks to the support point O is

$$d\vec{N} = \sum_{n=1}^{n}(z_n\vec{k}\times d\vec{P}_n) = [(\dot{\omega} + (\omega^2\vec{k}\times)]\sum_{n=1}^{n}(z_n\vec{s}_n dm_n) \quad (6)$$

By integrating (5) and (6), we can obtain unbalanced force and unbalanced moment

$$P = \int dP = [(-\dot{\omega}\vec{k}\times) + \omega^2]\sum_{n=1}^{n}\int\vec{s}_n dm_n \quad (7)$$

$$N = \int dN = [\dot{\omega} + (\omega^2\vec{k}\times)]\sum_{n=1}^{n}\int z_n\vec{s}_n dm_n \quad (8)$$

Among (7) and (8),

$$\int\vec{s}_n dm_n = (\int x_n dm_n)\vec{i} + (\int y_n dm_n)\vec{j} = M_n\vec{e}_n \quad (9)$$

$$\int z_n\vec{s}_n dm_n = (\int z_n x_n dm_n)\vec{i} + (\int z_n y_n dm_n)\vec{j} = I_{z_n x_n}\vec{i} + I_{y_n z_n}\vec{j} \quad (10)$$

In (9) and (10), $\vec{e}_n = \vec{s}_n = x_n\vec{i} + y_n\vec{j}$ is the eccentricity of each disk and $I_{z_n x_n}$, $I_{y_n z_n}$ are the inertia products on the z-x and y-z axis.

The unbalanced force and unbalanced moment can be obtained

$$P = [(-\dot{\omega}\vec{k}\times) + \omega^2]\sum_{n=1}^{n}M_n e_n \quad (11)$$

$$N = [\dot{\omega} + (\omega^2\vec{k}\times)]\sum_{n=1}^{n}(I_{z_n x_n}\vec{i} + I_{y_n z_n}\vec{j}) \quad (12)$$

Noting that unbalanced force $P = 0$, that is $e = 0$, the state is the static balanced state. Also, there is still an unbalanced moment N, when the unbalanced force couple N = 0, that is, $I_{z_n x_n} = 0$ and $I_{y_n z_n} = 0$. This condition can be considered no unbalanced vibration when the dynamic load becomes 0.

III. DESIGN OF SQP OPTIMIZATION

There is a nonlinear relationship between unbalanced force and unbalanced moment with their interfering factors. In this paper, SQP algorithm is used to predict the assembly phase of the multistage disks of the tie rod rotor system. This algorithm is suitable for the multidimensional nonlinear constraint minimum optimization problem, and it has good convergence, high calculation efficiency, boundary search abilities, strong global optimization capabilities.

The basic idea of SQP algorithm is to simplify an objective nonlinear programming problem into a quadratic programming problem at an approximate solution. Determine a gradient descent direction and calculate iteratively to solve the problem. The step of current iteration point is obtained by reducing the value function. Finally, the global optimal solution can be solved [27]–[30].

Determine the objective function as follows

$$\text{Objective function: } \min f(X) \quad (13)$$

The constraint functions can be determined by

$$s.t.g_u(X) \le 0(u = 1, 2, \cdots, p) \quad (14)$$

$$h_v(X) = 0(v = 1, 2, \cdots, m) \quad (15)$$

The Taylor Formula can simplify the objective function into a quadratic function at the iteration point X_k. And the constraint functions are simplified to linear functions. Based on the above simplification, the nonlinear problem is transformed into a quadratic programming problem:

$$\begin{aligned}&\min\\ &f(X) = \frac{1}{2}[X - X_k]^T\nabla^2 f(X_k)[X - X_k] + \nabla f(X_k)^T[X - X_k]\\ &s.t.\nabla g_u(X_k)^T[X - X_k] + g_u(X_k) \le 0(u = 1, 2, \cdots, p)\\ &\nabla h_v(X_k)[X - X_k] + h_v(X_k) = 0(v = 1, 2, \cdots, m)\end{aligned} \quad (16)$$

The (16) is the approximation problem of the optimization problem under the original constraint. When $S = [X - X_k]$, we can obtain:

$$\begin{aligned}&\min f(X) = \frac{1}{2}S^T\nabla^2 f(X_k)S + \nabla f(X_k)^T S\\ &s.t.\nabla g_u(X_k)^T S + g_u(X_k) \le 0(u = 1, 2, \cdots, p)\\ &\nabla h_v(X_k)S + h_v(X_k) = 0(v = 1, 2, \cdots, m)\end{aligned} \quad (17)$$

In (17), define the letters as follows

$$\begin{aligned}H &= \nabla^2 f(X_k)\\ C &= \nabla f(X_k)\\ A_{eq} &= [\nabla h_1(X_k), \cdots, \nabla h_m(X_k)]^T\\ A &= [\nabla g_1(X_k), \cdots, \nabla g_P(X_k)]^T\\ B_{eq} &= [h_1(X_k), \cdots, h_m(X_k)]^T\\ B &= [g_1(X_k), \cdots, g_P(X_k)]^T\end{aligned} \quad (18)$$

The quadratic problem is simplified to a general form

$$\min\frac{1}{2}S^T HS + C^T S$$

$$s.t.AS \leq B$$
$$A_{eq}S = B_{eq} \tag{19}$$

The approximate calculation of the second derivative matrix H is calculated using the variable-scale matrix in the quasi-Newton method

$$H_{k+1} = H_k + \frac{\Delta X_k[\Delta X_k]^T}{[\Delta q_k]^T \Delta X_k} - \frac{H_k \Delta q_k [\Delta q_k]^T H_k}{[\Delta q_k]^T H_k \Delta q_k} \tag{20}$$

Using the Lagrange transformation on (19) can obtain

$$\min L(S, \lambda) = \frac{1}{2} S^T H S + C^T S + \lambda^T (A_{eq} S - B_{eq}) \tag{21}$$

Set the extreme condition of (21) to $\nabla L(S, \lambda) = 0$

$$\begin{bmatrix} H & A_{eq}^T \\ A_{eq} & 0 \end{bmatrix} \begin{bmatrix} S \\ \lambda \end{bmatrix} = \begin{bmatrix} -C \\ B_{eq} \end{bmatrix} \tag{22}$$

The solution can be obtained as $[S_{k+1}, \lambda_{k+1}]^T$, if the multipliers corresponding to the original constraints are not all 0. Then the multipliers corresponding to the active constraints are not less than 0. And S_{k+1} is the optimal solution S^* of the quadratic programming problem.

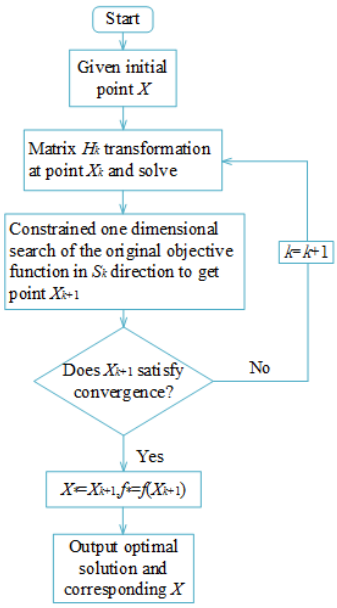

FIGURE 4. Flow chart of SQP algorithm.

As shown in Fig. 4, the iterative steps of SQP algorithm are as follows:

Step 1: Determine the parameters including initial point X_0 and the constraint functions.

Step 2: Perform matrix H_k transformation at point X_k and one-dimensional search the point X_{k+1} on the objective function.

Step 3: Determine the termination criterion for the point X_{k+1}. If X_{k+1} meets the termination criterion, $X^* = X_{k+1}$, $f^* = f(X_{k+1})$, and output the minimum value and corresponding X value of the objective function. Otherwise, enter the block diagram again and calculate from the beginning.

Step 4: Correct H_{k+1} again, set $k = k + 1$, and continue iterating until the X_n meets the termination criterion.

IV. OPTIMAL STRATEGY

For the tie rod rotor studied in this paper, the multistage disks are connected by eight tie rod bolts, so the angle between every two bolt holes is 45°. The optimal strategy aims to obtain the phase of the multistage disks to meet the minimum value of unbalanced force and unbalanced moment of the system. Thus, the optimal strategy is shown as follows.

The optimization for unbalanced force is given in (23)

$$F^{SQP}(\theta_F) = \min\{\sqrt{(\sum_{i=1}^{n} M_n R_n \cos\theta_n \omega^2)^2 + (\sum_{i=1}^{n} M_n R_n \sin\theta_n \omega^2)^2}$$
$$sub.to: 0 \leq \theta_n \leq 2\pi \tag{23}$$

The optimization for unbalanced moment is given in (24)

$$F^{SQP}(\theta_N) = \min\{\sqrt{(\sum_{i=1}^{n} M_n R_n \cos\theta_n z_n \omega^2)^2 + (\sum_{i=1}^{n} M_n R_n \sin\theta_n z_n \omega^2)^2}$$
$$sub.to: 0 \leq \theta_n \leq 2\pi \tag{24}$$

where M_n and R_n are the unbalanced mass and counterweight radius of each disk, respectively. θ_n is the optimal assembly phase of each disk. z_n represents the distance from each disk to the support.

V. EXPERIMENT VALIDATION

A. EXPERIMENTAL SETUP

In order to verify the vibration control effect on unbalanced force and unbalanced moment of the tie rod rotor optimized by the SQP algorithm, the schematic diagram of the platform is shown in Fig. 5. As can be seen, the platform consists of

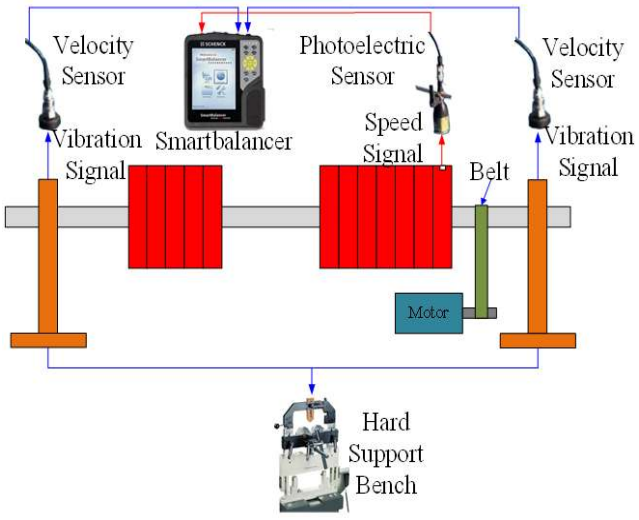

FIGURE 5. A schematic view of a platform.

a base, an acquisition processing analysis system and tie rod rotor. The base is a schenck hard-support dynamic balancing machine with a total length of 5m and voltage of 380V. There are 10 movable hard supports which can be used to support the rotor structure with a shaft diameter of 9 to 140mm. Schenck also has two drive modes including belt drive and gimbal drive. This paper uses a belt drive which rotates 0 to 1000rpm. And in this experiment, the transmission ratio is 1:10, that is, the speed range of rotor system is 0 to 10000rpm. The platform has a protective cover, divided into three parts, which can completely cover the whole rotor system to ensure the safety of process.

The acquisition processing analysis system includes a smartbalancer dynamic balancer, a photoelectric sensor and two vibration speed sensors which can display imbalance vector diagrams, single-plane and dual-plane dynamic balancing with different kinds of rotors and hammer test modules. The analysis system has a balancing speed with 120rpm to 60000rpm and a weight accuracy with 0.1g. The photoelectric sensor is used to measure the rotation speed of the rotor. The measurement distance can reach 2m with a 0.5Hz to 40kHz measurement frequency range. Also, the sampling frequency of each channel is up to 131kHz. The vibration speed sensor can measure the Peak to Peak value of the vibration speed up to 6000 mm/s $\pm 1\%$, and the sensitivity reaches 100mV/g. These experimental devices can meet the experimental demands.

The initial imbalance of each disk can be measured by the acquisition processing analysis system. The test steps are as follows:

(1) Number all the disk. Noting that two of the disks are connected by a transition shaft. The numbers are 1 to 11.

(2) Reflective tape on the left disk near the belt drive is used to measure the speed. The default phase is 0° which is set as a reference.

(3) Perform single-plane dynamic balancing to obtain the imbalance of each disk. And the counterweight radius is 62mm of all the disks.

The imbalance amount is presented by mass-diameter product W which can be calculated by (25)

$$W = M_n \cdot R_n \tag{25}$$

The imbalance parameters of each disk can be seen in Table 1. We can assemble multistage disks for optimization experiment.

TABLE 1. Imbalance of each disk.

Number	Imbalance amount (g·m)	Imbalance phase (°) [a]
1	0.0806	231
2	0.7874	2
3	0.2604	350
4	0.2914	182
5	0.3224	325
6	0.4402	167
7	0.2914	354
8	0.4712	358
9	0.5704	349
10	0.4278	12
11	0.3286	3

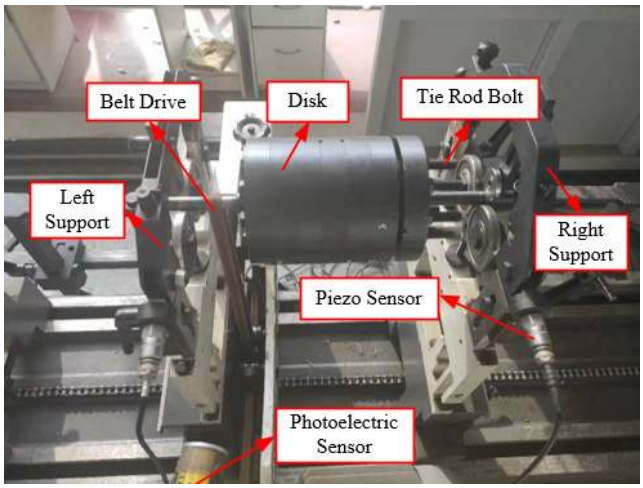

FIGURE 6. Ordinary multistage disk tie rod rotor platform.

B. EXPERIMENT RESULTS

In this experiment, disk marked with numbers 1, 3, 4, 5, 7, 8, and 11 are bolted together to set up an ordinary multistage disk tie rod rotor. This experiment is a comparative experiment. Compared with the random assembly of the disk phase, at 1200 r/min, the vibration amplitude of the left and right support is 1.426 mm/s∠189° and 1.668 mm/s∠192°. And then perform on the seven-stage disks with unbalanced force and unbalanced moment optimization respectively. The experimental results compared with initial vibration can be seen in Fig. 7 and Table 2.

It can be found from Fig. 7 and Table.2 that both unbalanced force optimization and unbalanced moment optimization have a good effect of vibration control on the left and right support. As for unbalanced force optimization, the vibration reduction of the left and right support is 49.56% and 50.95%. On the other hand, the vibration of the left and right support reduces 51.40% and 56.59% respectively by using unbalanced moment optimization. In conjunction with Fig. 7 and Table. 2 can be seen that unbalanced moment

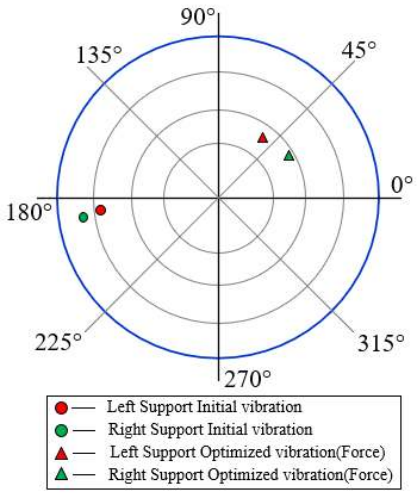

(a)

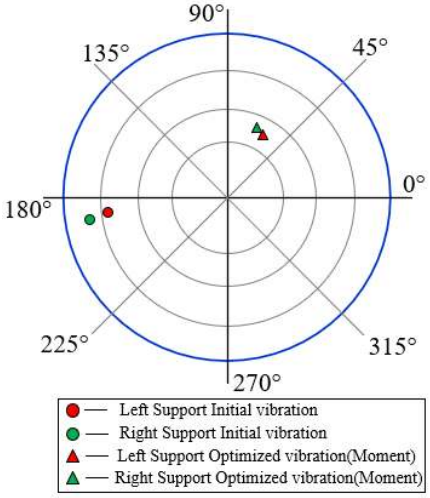

(b)

FIGURE 7. Two optimization methods of tie rod rotor.

TABLE 2. Vibration of each support.

Assembly method	Left support vibration (mm/s)	Right support vibration (mm/s)
Random	1.426 mm/s∠189°	1.668 mm/s∠192°
Force optimization	0.719 mm/s∠48°	0.818 mm/s∠35°
Moment optimization	0.693 mm/s∠56°	0.724 mm/s∠60°

optimization is better than unbalanced force optimization in the aspect of vibration control.

As can be known, unbalanced moment optimization is a better method for vibration control. Therefore, it is applied to the platform of a gas turbine tie rod rotor structure as shown in Fig. 8. The structure is more complicated than the structure in Fig. 6. It consists of compressor end and turbine end, both

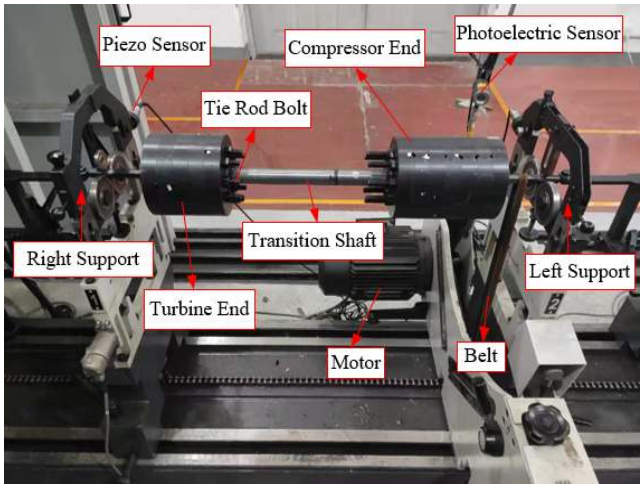

FIGURE 8. Gas turbine tie rod rotor structure platform.

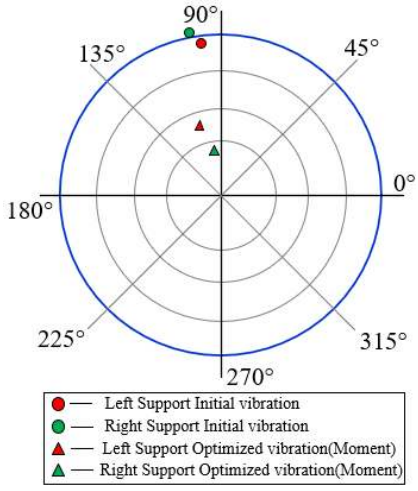

FIGURE 9. Unbalanced moment optimization at constant speed.

TABLE 3. Vibration of each support.

Assembly method	Left support vibration (mm/s)	Right support vibration (mm/s)
Random	1.941 mm/s∠103°	2.011 mm/s∠106°
Moment optimization	0.766 mm/s∠117°	0.469 mm/s∠94°

parts are connected by the tie rod bolts. In order to verify the effect of unbalanced moment optimization in the gas turbine rotor, set two conditions including constant speed test and speed-up test which passes the critical speed.

At the speed of 1200r/min with a random assembly of disks. In Fig. 9 and Table.3, the both vibration values are 1.941 mm/s∠103° and 2.011 mm/s∠106 °, respectively.

As shown in Fig. 9 and Table. 3, the unbalanced moment optimization has a vibration control effectively. There are 0.766 mm/s∠117° and 0.469 mm/s∠94° on the left and right

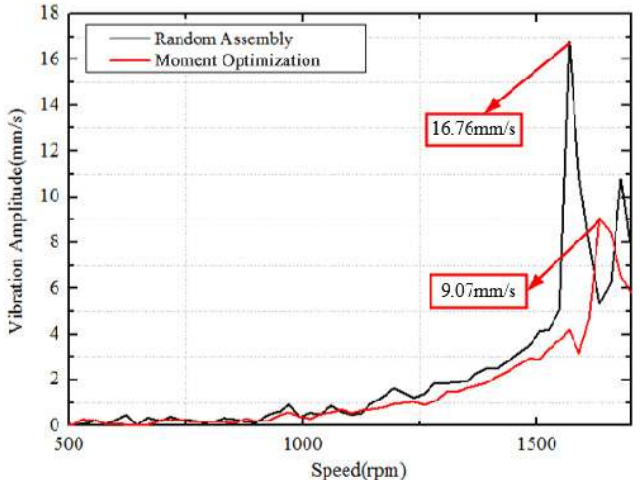

FIGURE 10. Amplitude-frequency characteristic curve of speed-up.

supports, respectively. Additionally, vibration reduction of every support is 60.54% and 76.68% compared with random assembly.

Then the speed-up experiment ranges from 500r/min to 1700r/min of the gas turbine tie rod rotor with unbalanced moment optimization is tested. The first-order critical speed can be passed in this experiment. As we all know, the critical speed has the biggest vibration within the test speed range. The amplitude-frequency characteristic curve can be obtained through the experiment as shown in Fig. 10.

Unbalanced moment optimization has a good vibration control before the critical speed, at the critical speed and after the critical speed in Fig. 10. The critical speed of random assembly is 1558r/min with a 16.76mm/s vibration value. Besides, there is a 9.07mm/s vibration value at a 1634r/min critical speed after unbalanced moment optimization. The latter method reduces 43.3% compared with the former method. The reasons for the slight difference in the critical speed of the two assemblies maybe that the random assembly makes the vibration relatively large which can loosen the tie rod bolts. The stiffness of gas turbine tie rod rotor system decreases. As a result, the critical speed is also reduced. However, with the optimization of unbalanced moment, the vibration can be controlled effectively that keeps the tie rod bolts tight. What is more, the stiffness of the system increases which can enhance the critical speed.

As can be seen in Fig. 10, there is a good vibration control with unbalanced moment optimization. It can provide some guidance for the actual assembly process of the gas turbine rotor.

VI. CONCLUSION

In this paper, aiming at the problem of unbalanced vibration of the gas turbine tie rod rotor system, a method based on SQP algorithm to optimize unbalanced force and unbalanced moment is proposed to predict the assembly phase of the multistage disks, so as to control the vibration of the system.

TABLE 4. Physical meaning of each letter.

Letter	Physical meaning
M_n	Disk unbalanced mass
z_n	Distance from disk to support
$\vec{r}_n$	Position of the imbalance on each disk
$\vec{s}_n$	Projection of $\vec{r}_n$ on the x-y plane
$\vec{v}_n$	Speed of disk unbalanced mass
ω	Tie rod rotor rotation speed
$\vec{a}_n$	Acceleration of disk unbalanced mass
P	Unbalanced force
N	Unbalanced Moment
e_n	Disk eccentricity
X_k	Iteration point
H	Second derivative matrix
S^*	Optimal solution
θ_n	Phase of optimization assembly disk
R_n	Counterweight radius of each disk

The factors in the unbalance problem of the rotor system are analyzed. Besides, unbalanced force and unbalanced moment of the system are mainly considered with a dynamic model. The prediction strategy of unbalanced force optimization and unbalanced moment optimization of the rotor system is established which is matched with SQP algorithm for optimization.

In order to verify the effectiveness of the proposed method, the experiments are carried out using an acquisition processing analysis system. The results show that compared with random assembly of multistage disks, both unbalanced force optimization and unbalanced moment optimization can control the vibration of rotor system. Additionally, the effect of unbalanced moment optimization is better. Furthermore, unbalanced moment optimization method is verified in a more complicated gas turbine tie rod rotor structure. Compared with random assembly at a speed of 1200r/min, the left and right support decreases 60.54% and 76.68%. During the speed-up processing which passes the critical speed, unbalanced moment optimization can achieve a vibration reduction of 43.3% at the critical speed.

On the one hand, the method obtained in this paper can play a guiding role in the assembly process of the gas turbine rotor system. On the other hand, it can ensure the safe and stable when the rotor is working. In the future, the influence of thermodynamic factors on the tie rod rotor system will be considered under a high temperature environment. Also, the model of unbalanced force and unbalanced moment jointly optimizing the gas turbine rotor will be taken into account.

APPENDIX

Physical meaning of each letter in the paper can be found in Table. 4.

ACKNOWLEDGMENT

The authors would like to thank the coauthors for their help and suggestions. The authors are also very grateful to the editors and the reviewers for their careful reading and helpful comments.

REFERENCES

[1] K. S. Hodgkinson, "Gas turbine aero engine rotor balance and vibration," *Aircr. Eng. Aerosp. Technol.*, vol. 36, no. 7, pp. 218–220, Jul. 1964.
[2] A. Pozarlik and J. B. Kok, "Numerical prediction of interaction between combustion, acoustics and vibration in gas turbines," *J. Acoust. Soc. Amer.*, vol. 123, no. 5, p. 3404, May 2008.
[3] B. D. Thompson, "Optimization of LM2500 gas generator and power turbine trim-balance techniques," *J. Eng. Gas Turbines Power*, vol. 114, no. 2, pp. 222–229, Apr. 1992.
[4] J. Chen, D. Jiang, and C. Liu, "Fault analysis and optimal balancing of bowing of steam turbine rotor under long-term service," *J. Eng. Gas Turbines Power*, vol. 137, no. 11, Nov. 2015, Art. no. 112503.
[5] A. Lifson, G. H. Quentin, A. J. Smalley, and C. L. Knauf, "Assessment of gas turbine vibration monitoring," *J. Eng. Gas Turbines Power*, vol. 111, no. 2, pp. 257–263, Apr. 1989.
[6] J. Liu, W. Wang, and F. Golnaraghi, "An enhanced diagnostic scheme for bearing condition monitoring," *IEEE Trans. Instrum. Meas.*, vol. 59, no. 2, pp. 309–321, Feb. 2010.
[7] X. Xu, Y. Lei, and Z. Li, "An incorrect data detection method for big data cleaning of machinery condition monitoring," *IEEE Trans. Ind. Electron.*, vol. 67, no. 3, pp. 2326–2336, Mar. 2020.
[8] E. E. Mangina, S. D. J. McArthur, J. R. McDonald, and A. Moyes, "A multi agent system for monitoring industrial gas turbine start-up sequences," *IEEE Trans. Power Syst.*, vol. 16, no. 3, pp. 396–401, Aug. 2001.
[9] A. Rizvi, C. W. Smith, R. Rajasekaran, and K. E. Evans, "Dynamics of dry friction damping in gas turbines: Literature survey," *J. Vibrat. Control*, vol. 22, no. 1, pp. 296–305, Jan. 2016.
[10] P. V. Ramaiah and G. Krishnaiah, "Modelling and design of friction damper used for the control of vibration in a gas-turbine blade–a microslip approach," *Proc. Inst. Mech. Eng. C, J. Mech. Eng. Sci.*, vol. 221, no. 8, pp. 887–895, Aug. 2007.
[11] S.-J. Huang and L.-C. Lin, "Fuzzy dynamic output feedback control with adaptive rotor imbalance compensation for magnetic bearing systems," *IEEE Trans. Syst., Man Cybern. B, Cybern.*, vol. 34, no. 4, pp. 1854–1864, Aug. 2004.
[12] J. Kejian, Z. Changsheng, and C. Liangliang, "Unbalance compensation by recursive seeking unbalance mass position in active magnetic bearing-rotor system," *IEEE Trans. Ind. Electron.*, vol. 62, no. 9, pp. 5655–5664, Sep. 2015.
[13] Y. Zheng, N. Mo, Y. Zhou, and Z. Shi, "Unbalance compensation and automatic balance of active magnetic bearing rotor system by using iterative learning control," *IEEE Access*, vol. 7, pp. 122613–122625, 2019.
[14] A. Looser, A. Tuysuz, C. Zwyssig, and J. W. Kolar, "Active magnetic damper for ultrahigh-speed permanent-magnet machines with gas bearings," *IEEE Trans. Ind. Electron.*, vol. 64, no. 4, pp. 2982–2991, Apr. 2017.
[15] H. Gao, X. Meng, and K. Qian, "The impact analysis of beating vibration for active magnetic bearing," *IEEE Access*, vol. 7, pp. 134104–134112, 2019.
[16] A. F. Storace, D. Sood, J. P. Lyons, and M. A. Preston, "Integration of magnetic bearings in the design of advanced gas turbine engines," *J. Eng. Gas Turbines Power*, vol. 117, no. 4, pp. 655–665, Oct. 1995.
[17] W. Deng, J. Yao, and D. Ma, "Time-varying input delay compensation for nonlinear systems with additive disturbance: An output feedback approach," *Int. J. Robust Nonlinear Control*, vol. 28, no. 1, pp. 31–52, Jan. 2018.
[18] C. Luo, J. Yao, and J. Gu, "Extended-state-observer-based output feedback adaptive control of hydraulic system with continuous friction compensation," *J. Franklin Inst.*, vol. 356, no. 15, pp. 8414–8437, Oct. 2019.
[19] W. Zhou, X. Wei, and L. Zhai, "Nonlinear characteristics and stability optimization of rotor-seal-bearing system," *J. Vibroeng.*, vol. 16, no. 2, pp. 818–831, Mar. 2014.
[20] C. Sun, C. Li, Y. Liu, Z. Liu, X. Wang, and J. Tan, "Prediction method of concentricity and perpendicularity of aero engine multistage rotors based on PSO-BP neural network," *IEEE Access*, vol. 7, pp. 132271–132278, 2019.
[21] H. Zhang, C. Zhang, Y. Peng, D. Wang, G. Tian, X. Liu, and Y. Peng, "Balancing problem of stochastic large-scale U-Type assembly lines using a modified evolutionary algorithm," *IEEE Access*, vol. 6, pp. 78414–78424, 2018.
[22] L. Tong, X. Li, J. Hu, and L. Ren, "A PSO optimization scale-transformation stochastic-resonance algorithm with stability mutation operator," *IEEE Access*, vol. 6, pp. 1167–1176, 2018.
[23] L. J. Cvetianin, "Balancing of flexible rotor with variable mass," *Mechanism Mach. Theory*, vol. 16, no. 5, pp. 507–516, Jan. 1981.
[24] F. Sève, M. A. Andrianoely, A. Berlioz, R. Dufour, and M. Charreyron, "Balancing of machinery with a flexible variable-speed rotor," *J. Sound Vibrat.*, vol. 264, no. 2, pp. 287–302, Jul. 2003.
[25] X. Xu and P. P. Fan, "Rigid rotor dynamic balancing by two-plane correction with the influence coefficient method," *Appl. Mech. Mater.*, vols. 365–366, pp. 211–215, Aug. 2013.
[26] D. J. Rodrigues, A. R. Champneys, M. I. Friswell, and R. E. Wilson, "Experimental investigation of a single-plane automatic balancing mechanism for a rigid rotor," *J. Sound Vibrat.*, vol. 330, no. 3, pp. 385–403, Jan. 2011.
[27] J. Che and K. Su, "A modified SQP method and its global convergence," *Appl. Math. Comput.*, vol. 186, no. 2, pp. 945–951, Mar. 2007.
[28] P. Li, J. Qi, J. Wang, H. Wei, X. Bai, and F. Qiu, "An SQP method combined with gradient sampling for small-signal stability constrained OPF," *IEEE Trans. Power Syst.*, vol. 32, no. 3, pp. 2372–2381, May 2017.
[29] Z. Wei, L. Qi, and X. Chen, "An SQP-type method and its application in stochastic programs," *J. Optim. Theory Appl.*, vol. 116, no. 1, pp. 205–228, Jan. 2003.
[30] N. I. M. Gould and D. P. Robinson, "A second derivative SQP method: Global convergence," *SIAM J. Optim.*, vol. 20, no. 4, pp. 2023–2048, Jan. 2010.

YIPENG ZHANG was born in 1995. He is currently pursuing the Ph.D. degree with the Department of Mechanical and Electrical Engineering, Beijing University of Chemical Technology, Beijing, China. His research interests include rotating machinery vibration control and optimization algorithm.

LIDONG HE was born in 1963. He received the Ph.D. degree from the Harbin Institute of Technology, Harbin, China. He has extensive engineering project experience in vibration control of rotating machinery and solved complex vibration problems for many enterprises. His research interests include rotating machinery and pipe vibration control.

JIANJIANG YANG was born in 1995. He is currently pursuing the M.Eng. degree with the Department of Mechanical and Electrical Engineering, Beijing University of Chemical Technology, Beijing, China. His research interest includes rotating machinery active vibration control.

JIAN WANG was born in 1996. He is currently pursuing the M.Eng. degree with the Department of Mechanical and Electrical Engineering, Beijing University of Chemical Technology, Beijing, China. His research interest includes pipe vibration control in petrochemical industries.

GANG ZHU was born in 1997. He is currently pursuing the M.Eng. degree with the Department of Mechanical and Electrical Engineering, Beijing University of Chemical Technology, Beijing, China. His research interests include rotating mechanical seal design and pipe vibration control.